An experimental and numerical analysis of natural convection in an air filled square cavity with an insulated baffle

G. Nardini, M. Paroncini, and R. Vitali

Abstract— An experimental and numerical analysis is carried out in an air filled square cavity. The cavity has the horizontal adiabatic walls and the vertical walls with discrete sources. An insulated baffle is attached to its horizontal wall between the hot sources.

The effect of baffle length is experimentally and numerically investigated for Rayleigh numbers in the range of 10^4 and 10^5. The dimensionless baffle lengths, L_b, are 0.2, 0.4 and 0.6. It is observed the influence of the baffle on the flow pattern and heat transfer. Interferograms, streamlines, isotherms, velocity maps are shown and heat transfer is analysed.

The results clearly demonstrate that the baffle has a significant effect on the heat transfer and flow characteristics of the fluid. The flow field pattern is baffle length and Rayleigh number dependent. It is, in fact, observed that the Nusselt number increases as Rayleigh number increases and always decreases increasing the baffle length. The average Nusselt numbers from $L_b = 0.2$ to $L_b = 0.6$ decreases on average by 13.9% on the lower source and 15.6% on the higher source.

Keywords— heat transfer, holographic interferometry, horizontal baffle, natural convection, square cavity

I. Introduction

NATURAL CONVECTION heat transfer in an air filled cavity has become very important in engineering systems because it affects the thermal performance in many industrial and engineering applications like heating and ventilating of rooms, insulation with double-pane windows solar collector systems, and cooling of electronic equipment. In many applications the baffle(s) are attached to the vertical or horizontal wall(s) of the cavity partitioning it. Many studies of natural convection in cavities are presented in technical literature and some of these studies find that both the size and position of the discrete heat source has a significant impact on natural convective heat transfer. Other studies find that the length and position of the baffle(s) have a significant effect on the heat transfer and flow characteristics of the fluid. Ho and Chang [1] numerically and experimentally investigated convective heat transfer in a vertical rectangular enclosure with two-dimensional discrete heating.

Tūrkoglu and Yūcel [2] numerically studied the effects of the heater and cooler location on natural convection in square cavities. Nithyadevi et al. [3] numerically investigated natural convection heat transfer in the cavities with partially active sides for different aspect ratios. Chu, Churchil et al. [4] computationally analysed the effect of heater size, location, aspect ratio and boundary conditions on two dimensional rectangular channels. Valencia and Frederick [5] numerically studied heat transfer in square cavities with partially active vertical walls. Zhao, Liu et al. [6] theoretically investigated natural convection induced by two discrete heating elements flush mounted to one vertical wall of a square cavity. Qi-Hong Deng [7] numerically analysed natural convection due to discrete source-sink pairs.

Paroncini et al. [8] experimentally and numerically analysed natural convective heat transfer in a square enclosure with partially active side walls. Regarding abaffle attached to the vertical wall, Bajorek et al. [9] carried out an experimental investigation of natural convection differentially heated air filled square portioned cavity. Jetli et al. [10] numerically analysed a differentially heated air filled square partitioned cavity with three different combinations of baffle position. Ambarita et al. [11] numerically investigated laminar natural convective heat transfer in a square cavity with two insulated baffles attached to its horizontal walls. Concerning baffles attached to the horizontal wall, Tasnim and Collins [12] numerically investigated heat transfer in a square cavity with a baffle on the hot wall, Frederick [13] studied natural convection in an inclined square enclosure with a partition attached to its cold wall, Facas [14] numerically investigated natural convection in a cavity with fins attached to both

G.Nardini is with the DIISM, Dipartimento di Ingegneria Industriale e Scienze Matematiche, Università Politecnica delle Marche, Via Brecce Bianche - 60131 Ancona, ITALY (corresponding author phone +390712204876, fax +390712204770, e-mail: g.nardini@univpm.it).

M.Paroncini., is with the DIISM, Dipartimento di Ingegneria Industriale e Scienze Matematiche, Università Politecnica delle Marche, Via Brecce Bianche - 60131 Ancona, ITALY (e-mail: m.paroncini@univpm.it).

R.Vitali is with the DIISM, Dipartimento di Ingegneria Industriale e Scienze Matematiche, Università Politecnica delle Marche, Via Brecce Bianche - 60131 Ancona, ITALY (e-mail: r.vitali@univpm.it).

vertical walls, Yamaguchi and Asako [15] the effect of wall partitions on natural convective heat transfer in a vertical air layer. Nag et al. [16], Shi and Khodadadi [17] numerically studied a differentially heated square cavity where a horizontal plate was attached on the hot wall. Ghassemi at al. [18] numerically investigated the effect of two insulated horizontal baffles placed at the walls of a differentially heated square cavity. Bilgen [19] carried out a numerical study of natural convection in cavities with a thin fin on the hot wall.

However, there are very few experimental contributions to natural convection in enclosures with multiple discrete heat sources with a horizontal baffle. In this paper an experimental and numerical analysis of a square cavity of side length H with four discrete sources of height H/4 (two hot ones kept at a temperature T_h that changes from one test to another to obtain different Rayleigh numbers and two cold ones maintained at a fixed temperature T_c) located on the vertical walls with a baffle will be carried out. The baffle is insulated, its dimensionless height is 0.18, its dimensionless length varies in the range from 0.2 to 0.6 and it is placed on left vertical wall between two heat sources. The effect of baffle length on the flow, temperature fields and heat transfer characteristics of the cavity will be investigated. The thermal behaviour of heat transfer is experimentally studied through holographic interferometry for baffle dimensionless lengths of 0.2 and 0.4 and numerically for all baffle lengths.

The experimental and numerical correlation connecting the Rayleigh numbers with the corresponding Nusselt numbers are analysed.

NOMENCLATURE

a = Thermal diffusivity [$m^2 \bullet s^{-1}$]
g = Modulus of the gravity vector [$m \bullet s^{-2}$]
k = Thermal conductivity [$W \bullet m^{-1} \bullet K^{-1}$]
H = Height cavity side [m]
Y_b = dimensionless height of baffle, h_b/H
L_b = dimensionless length of baffle, l_b/H
h_b = baffle height [m]
l_b = baffle length [m]
l = Heat source length [m]
L = Cavity depth in the experimental tests [m]
$\overline{Nu}$ = Average Nusselt number of the heat source
Nu_h = Local Nusselt number
Nu_{ave} = Average Nusselt number
Nu_{higher} = average Nusselt number of the higher source
Nu_{lower} = average Nusselt number of the lower source
Pr = Prandlt number
Ra = Rayleigh number
T = Temperature [K]
ΔT = Temperature difference between hot and cold strips [K]
x = Cartesian axis direction [m]
X = Dimensionless Cartesian axis direction
y = Cartesian axis direction [m]
Y = Dimensionless Cartesian axis direction

Greek symbols

β = Thermal expansion coefficient [K^{-1}]
ε = Dimensionless length of the heat source
θ = Dimensionless temperature
ρ = Density [$kg \bullet m^{-3}$]
υ = Kinematic viscosity [$m^2 \bullet s^{-1}$]

Subscripts

c = Cold wall
cal= Calculated data
exp = Experimental data
h = Hot wall
num = Numerical data

II. Experimental analysis

The physical model being considered is natural convection in a square cavity of side length H with four sources of height size H/4 located on the vertical walls. The cavity is a square transversal section with a length in the longitudinal direction (L = 8.1•H) that is much greater than H to let the motion develop along the z axis, parallel to the laser beam, with a two-dimensional shape. Three baffle lengths are considered. The baffle is attached to the left vertical wall between the two hot sources. It is insulated and its Y_b is 0.18 and L_b varies in the range from 0.2 to 0.6. A schematic of the cavity and its coordinate system are shown in Fig. 1.

Cold sources are maintained at a fixed temperature T_c (291.16 K), and heat sources are kept at a temperature T_h, that changes from one test to another to obtain different Rayleigh numbers. The heat sources are an aluminum pipe with a rectangular transversal section that is flush mounted on the lateral walls of the cavity. The surfaces of the cavity are in Plexiglas.

The experimental set up is composed of a test cell filled with air at atmospheric pressure, a thermal system (two thermostatic baths, thermal circuit and temperature control system), a pneumatic auto-levelling table, a laser source, all of the necessary optical instrumentation and an acquisition system. The cavity is filled with air (Pr = 0.71) at atmospheric pressure, a room temperature of 295 K and a relative humidity of 50 %.

The horizontal walls are in Plexiglas to prevent heat leakage through these walls. The vertical walls are composed of Plexiglas and crossed by four aluminium channels connected to two thermostatic baths, which provide the circulation of the heating and cooling fluid to maintain the strips at temperatures of T_c and T_h. However, because this is not feasible in the experimental analysis, the boundary condition at these surfaces was implemented to take into account the conductive heat flux through the Plexiglas walls.

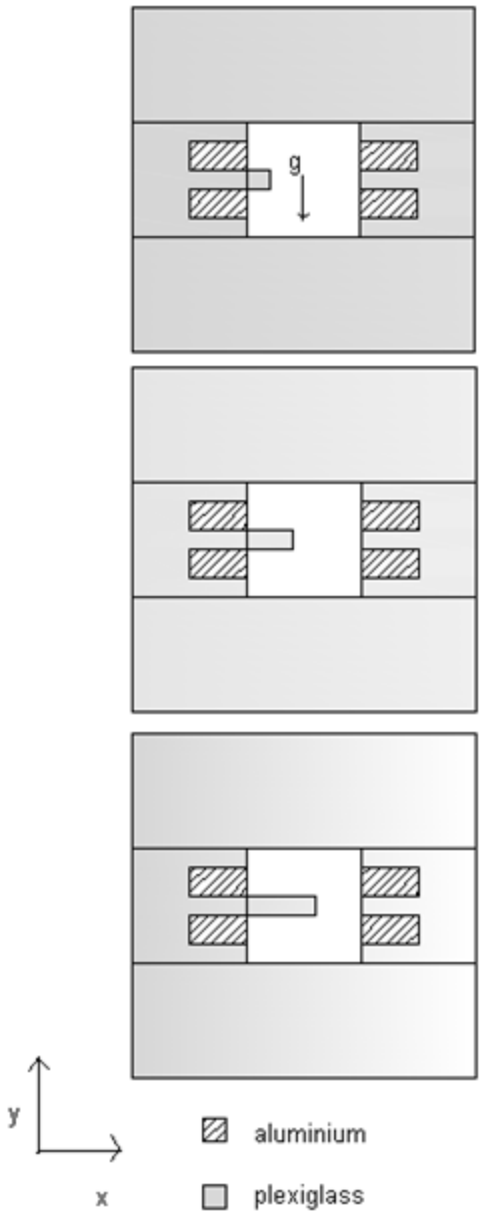

Fig. 1 The cavity with $L_b = 0.2$, $L_b = 0.4$ and $L_b = 0.6$

The thermostatic circuit is composed of two thermostats with their respective connecting pipes. The PROLINE RP1840 and RC20 thermostats are manufactured by Lauda Company. Each pipe connecting the thermostats with the inlet and outlet valves of the two sidewalls and heater are covered with a neoprene skin (approximately 0.02 m thick) to insulate them from heat loss. The thermostatic fluid is a mixture of 75 % water and 25 % glycol.

The acquisition system is composed of thirteen copper-constantan thermocouples located 1 mm under the surface of the test volume and are fixed through conductive paste. In each source, three thermocouples are inserted along the middle axis to measure the surface temperatures.

The thermocouples are connected to an ice point reference made by Kaye, model K170. Unfortunately, these temperatures cannot be used directly to obtain the temperature distribution of the fringes during the interpretation of the interferograms because, due to diffraction effects, the positions of both the heater and sidewalls are uncertain. For this reason, the last thermocouple is positioned in the middle of the air region to provide a reference temperature for the analysis of interferograms. The laser used is a ‘‘Model 532-400 DPSS’’ laser, a diode-pumped, frequency-doubled Nd:YAG laser that emits an output beam at a wavelength of 532 nm (green).

The analysis of the convective heat transfer phenomenon is conducted with a real-time and double-exposure technique.

The real-time technique is used to reveal the presence of plume oscillations and to study the temporal evolution of transfer processes, whereas the double-exposure technique is used for steady-state measurements. Holographic interferometry shows the typical advantages over classical optical techniques, such as high precision and sensitivity, very low noise level, and the possibility of displaying the temperature distribution across the whole investigated region. The interferograms are analysed with a traveling microscope to obtain the intensity distribution.

The density and temperature distribution are obtained by the usual methods of inversion. According to Hauf and Grigull [20], the expected accuracy for small fringe numbers (less than 30) can be approximately 10 %.

III. Numerical analysis

The numerical simulation is developed by Fluent 12.1.4, a finite volume code using the Boussinesq approximation for air and is performed with a 2d approximation [21].

The numerical results are carried out for $10^4 < Ra < 10^5$, and then compared to the experimental data. In this study, a second order upwind implicit scheme is employed in the conservation equations as it happens for the spatial discretization. The pressure interpolation is provided by the Body Force Weighted scheme; the pressure velocity coupling is provided by the SIMPLE algorithm, and a two-dimensional model is used with the condition of laminar flow. The diffusion terms are central-differenced with a second order accuracy.

The test cell is reproduced with real dimensions. The temperatures of the heated strips are assigned in order to obtain the same Rayleigh numbers as in the experimental analysis. The top and bottom surfaces are modelled to have conductive heat flux through the plexiglas walls.

The numerical average Nusselt numbers $\overline{Nu}$ on the heating elements are given by

$$\overline{Nu} \quad \frac{q_{tot} \cdot A_h}{k \cdot \Delta T \cdot A_H} \qquad (1)$$

where q_{tot} is the heat transfer rate directly computed by Fluent, A_h is the heater surface that is considered, and k is the thermal conductivity of the air evaluated at the heating strips temperature.

The local Nusselt numbers (Nu_h) are also referred to the heat source, and they are calculated as

$$Nu_h \quad \frac{c}{k \cdot \Delta T \cdot A_H} \qquad (2)$$

where q" is the heat flux computed by Fluent on each cell of the mesh.

IV. Results and Discussion

To understand the effects of the presence of baffles with different lengths, L_b = 0.2, L_b = 0.4 and L_b = 0.6 are considered. The Rayleigh number varies from 10^4 to 10^5 and the fluid inside cavity is dry air with Pr = 0.71. Flow and temperature fields along with heat transfer in the cavity are analysed.

A. Flow and temperature fields

Some examples of experimental and numerical flow and temperature field for L_b = 0.2 and L_b = 0.4 are presented in Fig. 2 and Fig. 3 whereas some examples of numerical flow and temperature fields for L_b = 0.6 are shown in Fig. 4. Figures are arranged going from top to bottom with ascending Ra numbers.

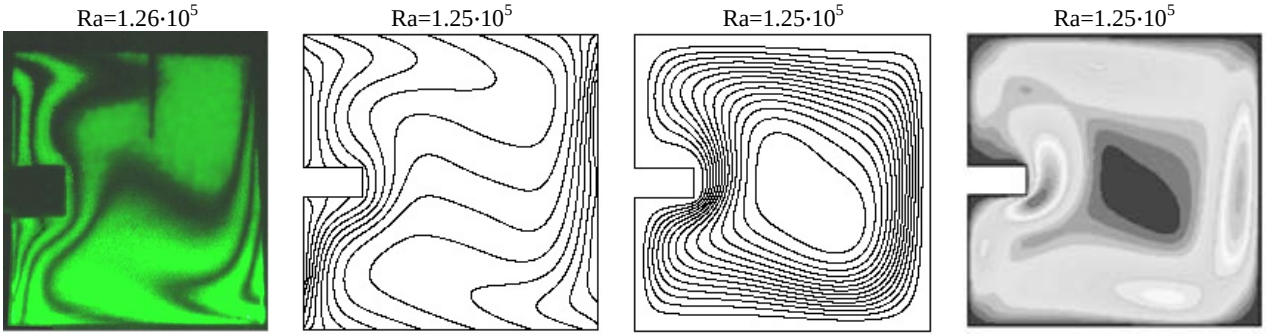

Fig. 2 Examples of the interferograms, streamlines, isotherms and velocity maps for L_b = 0.2

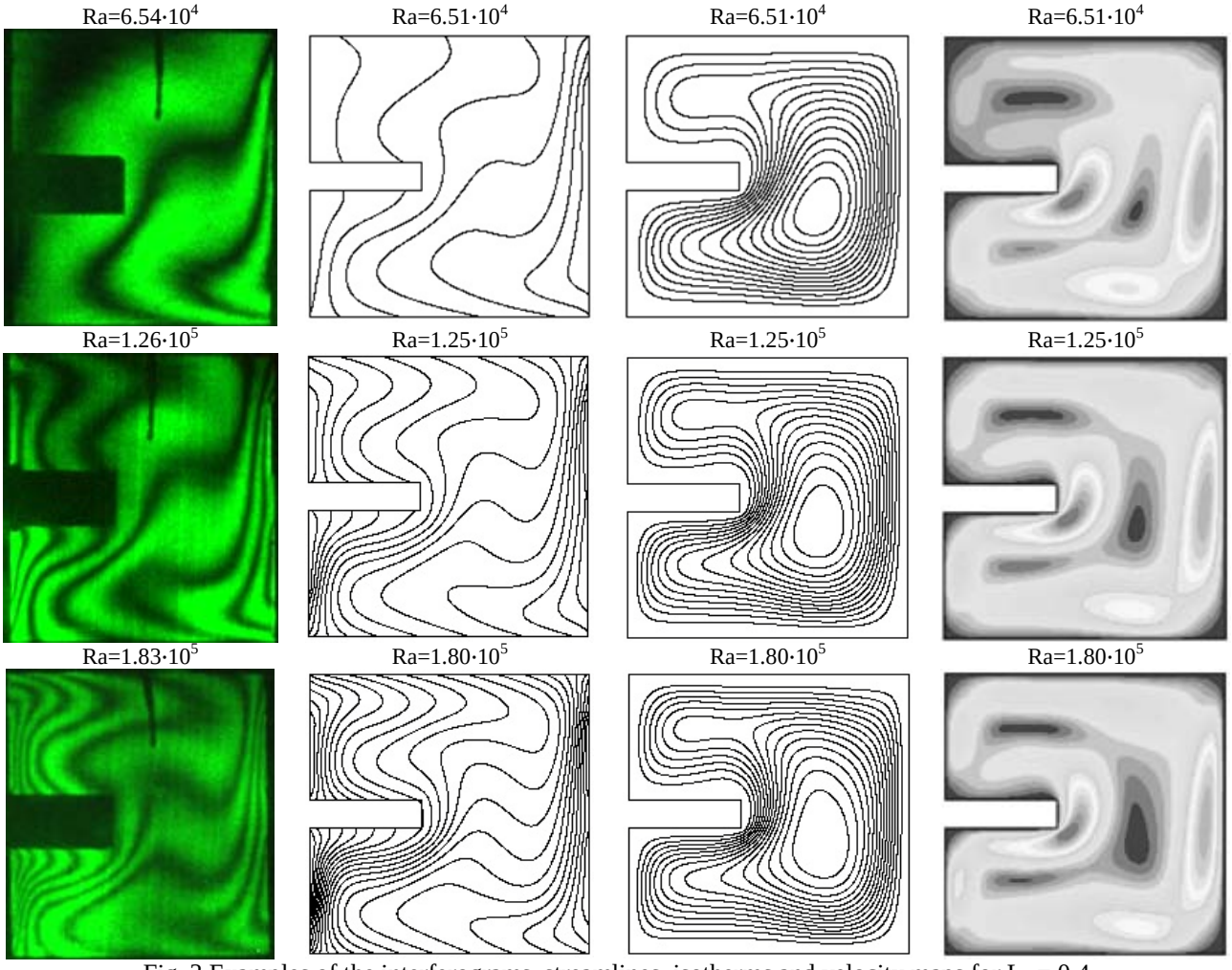

Fig. 3 Examples of the interferograms, streamlines, isotherms and velocity maps for L_b = 0.4

Ra=6.51·10^4 Ra=6.51·10^4 Ra=6.51·10^4

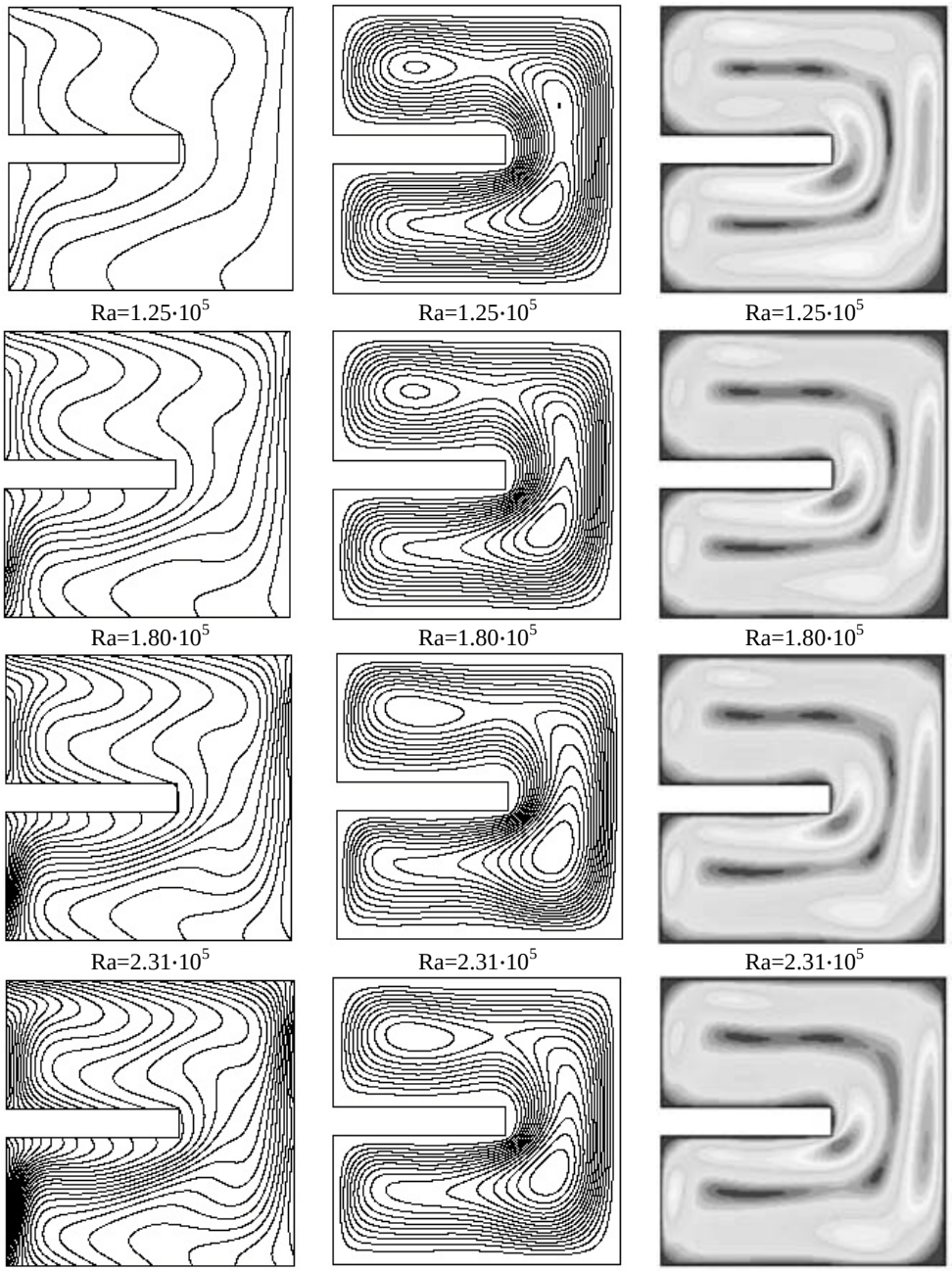

Fig. 4 Examples of the streamlines, isotherms and velocity maps for $L_b = 0.6$

Observing Fig. 2, 3 and 4 it is possible to note that the fringes in the high and low portions of the cavity are not perpendicular to the horizontal surface, showing that the top and bottom of the enclosure is not perfectly adiabatic. In Fig. 2, 3 and 4 it is possible to observe the temperature fields are modified for different baffle lengths.

By observing all the cases, it is found that the flow fields can be divided into two different patterns. The first pattern is the fluid circulation that creates a large clockwise rotating cell as shown in Fig. 2 and 3 for the baffles with $L_b = 0.2$ and $L_b = 0.4$. The fluid that is heated next to left wall rises and replaces the cooled fluid next to the right wall that is falling, thus gives rise to a clockwise rotating vortex shifted towards the right side wall by the baffle. For $L_b = 0.4$ the clockwise rotating cell is strangled by the baffle; it becomes smaller than the one for $L_b = 0.2$ and it is shifted even more to the right side of the cavity. The second pattern is the fluid separated into two different vortexes. In fact for $L_b = 0.6$, Fig. 4, two clockwise rotating cells are observed: one shifted to the right side wall above the bottom of the cavity and the other shifted to the left side wall above the baffle. This is because natural convection is more vigorous in the top left and bottom right of the cavity.

Another feature of these temperature patterns is that the streamlines become more packed next to the sidewall as the Ra increases for all L_b values. This suggests that the flow moves faster as natural convection intensifies. The maximum absolute value of the stream function can be viewed as a measure of the intensity of natural convection in the cavity. As the Ra increases, the maximum absolute value of the stream function increases. It is already possible to see a good

qualitative agreement between the numerical and the experimental temperature distribution in the cavity for L_b = 0.2 and L_b = 0.4 as confirmed by the Nusselt numbers.

B. Heat transfer

In order to evaluate how the presence of the baffle and its length affect heat transfer in the cavity, the average Nusselt numbers will be discussed. The experimental and numerical average Nusselt numbers as a function of Rayleigh number are shown in Tables 1 and 2 for Ra in the range from 10^4 to 10^5.

The Rayleigh numbers are defined as:

$$Ra = \frac{g\beta(T_h - T_c)H^3}{\nu\alpha} \quad (3)$$

The dimensionless parameters used are:

$$X = \frac{x}{H};\ Y = \frac{y}{H};\ \theta = \frac{(T-T_c)}{(T_h-T_c)};\ \varepsilon = \frac{1}{H} \quad (4)$$

The local Nusselt number – Nu(Y) –on the hot sources is calculated using the expression:

$$Nu_h(Y) = -\frac{\partial\theta}{\partial X}\Big|_{X=0} \quad (5)$$

The average Nusselt number - Nu_{ave} - on the heat sources is given by the relation:

$$Nu_{ave} = \frac{1}{\varepsilon}\int_0^{\varepsilon} Nu_h(Y)\,dY \quad (6)$$

The heat transfer rate for each source across the whole cavity is described by the average Nusselt number.

Table I Experimental Nusselt numbers for L_b = 0.2 and L_b = 0.4

L_b = 0.2			L_b = 0.4		
Rayleigh Number	**Higher source**	**Lower source**	**Rayleigh Number**	**Higher source**	**Lower source**
Ra	Nu	Nu	Ra	Nu	Nu
6.55E+04	1.75	2.81	6.54E+04	1.57	2.63
7.83E+04	2.03	3.25	7.83E+04	1.80	3.22
9.15E+04	2.22	3.64	9.15E+04	2.02	3.45
1.26E+05	2.81	4.46	1.26E+05	2.56	4.05
1.41E+05	2.85	5.01	1.41E+05	2.79	4.85
1.61E+05	3.07	5.52	1.61E+05	2.84	5.29
1.83E+05	3.10	5.97	1.83E+05	2.85	5.75
2.35E+05	3.91	7.42	2.34E+05	3.10	6.76

Table II Numerical Nusselt numbers for L_b = 0.2, L_b = 0.4 and L_b = 0.6

L_b = 0.2			L_b = 0.4			L_b = 0.6		
Rayleigh Number	**Higher source**	**Lower source**	**Rayleigh Number**	**Higher source**	**Lower source**	**Rayleigh Number**	**Higher source**	**Lower source**
Ra	Nu	Nu	Ra	Nu	Nu	Ra	Nu	Nu
6.51E+04	1.71	3.24	6.51E+04	1.4	2.67	6.51E+04	1.15	2.4
1.25E+05	2.77	5.35	1.25E+05	2.6	4.91	1.25E+05	2.46	4.64
1.80E+05	3.4	6.59	1.80E+05	3.18	6.14	1.80E+05	2.98	5.9
2.31E+05	3.82	7.44	2.31E+05	3.59	6.98	2.31E+05	3.41	6.76
2.78E+05	4.15	8.09	2.78E+05	3.98	7.63	2.78E+05	3.87	7.42
3.22E+05	4.41	8.62	3.22E+05	4.17	8.17	3.22E+05	4.05	7.95
3.98E+05	4.8	9.4	3.98E+05	4.62	8.96	3.98E+05	4.52	8.72

As shown in Tables I and II the Nusselt number is a function of baffle length. In fact the average Nusselt numbers on the hot sources decrease with the increase of baffle length from L_b = 0.2 to L_b = 0.6.

A relation between the average Nusselt numbers and the corresponding Rayleigh numbers is also elaborated.

This relation is:

$$Nu_{cal} = a \cdot Ra^b \quad (7)$$

The values of the parameters and correlation coefficients R^2 of equation 7 are shown in Tables III, IV and V.

R^2 is an indicator that describes the fitting of the function to the experimental data, and is defined as follows:

$$R^2 = 1 - \frac{SSE}{SST} \quad (8)$$

where

$$SST = (\sum_{j=1}^{n} k_j^2 + \frac{1}{n}(\sum_{i=1}^{n} k_i)^2 \quad (9)$$

and

$$SSE = \sum_{j=1}^{n}(k_j - h_j) \quad (10)$$

k_js are the n experimental values and h_js are the corresponding calculated value.

Table III Experimental and numerical correlation parameters

L_b = 0.2						
	Experimental correlation parameters			Numerical correlation parameters		
	a	b	R^2	a	b	R^2
higher source	0.0036	0.5608	0.933	0.0035	0.5651	0.983
lower source	0.0007	0.7479	0.998	0.0054	0.5827	0.982

Table IV Experimental and numerical correlation parameters

L_b = 0.4						
	Experimental correlation parameters			Numerical correlation parameters		
	a	b	R^2	a	b	R^2
higher source	0.0036	0.554	0.94	0.0012	0.6432	0.968
lower source	0.002	0.657	0.97	0.002	0.6573	0.972

Table V Experimental and numerical correlation parameters

L_b = 0.6

Numerical correlation parameters			
	a	b	R^2
higher source	0.0004	0.7312	0.956
lower source	0.0011	0.7014	0.968

Fig. 5 shows Nusselt numbers as a function of Rayleigh numbers for different baffle length.

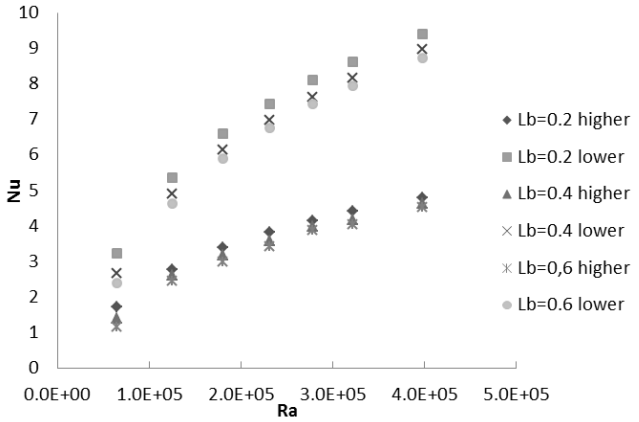

Fig. 5 Nusselt numbers with $L_b = 0.2$, $L_b = 0.4$ and $L_b = 0.6$

Observing Tables III, IV and V, it is possible to note that the growing Rayleigh numbers create a progressive development of the natural convective heat transfer indicated through the growing Nusselt numbers. Analysing Fig. 5 it is possible to note that for Ra = 104 the average Nusselt numbers are very small compared to the other values. The lower source has the higher heat transfer coefficient. This fact is due to the upward moving plume from the lower source that impinges on the higher source and affects its heat transfer characteristics. The fact that the fluid arriving at the higher source is in motion means that the higher source is situated in what appears to be forced convective flow. On the other hand, the heat transfer at the lower source tends to increase the temperature of the fluid that reaches the higher source with a value that is higher than the one of the ambient fluid. Consequently the buoyancy plume from the lower source decreases the heat flux of the higher source. Different baffle lengths modify the flow, temperature fields and heat transfer characteristics of the cavity as demonstrated in Fig. 5. In fact, from Lb = 0.2 to Lb = 0.4, the average Nusselt number decreases on average by 7.98% at the higher source and by 8.66% at the lower source; from Lb = 0.4 to Lb = 0.6 the average Nusselt number decreases on average by 6.77% at the higher source and by 4.67% at the lower source and from Lb = 0.2 to Lb = 0.6 the average Nusselt number of decreases on average by 15.67% at the higher source and by 13.9% at the lower source.

These values suggest that baffle length has a significant effect on the heat transfer and flow characteristics of the fluid.

V. Conclusions

Heat transfer by natural convection in a square cavity with four discrete sources of height H/4 is investigated for Rayleigh numbers in the range of 10^4 and 10^5. The effect of different baffle lengths attached to its vertical wall between the hot sources is experimentally and numerically investigated.

The baffle is perfectly insulated, its dimensionless height is $Y_b = 0.18$, its dimensionless length changes in the range from $L_b = 0.2$ to $L_b = 0.6$.

Different baffle lengths modify the flow and the temperature in the cavity. The flow field pattern is baffle length and Rayleigh number dependent.

It can be observed, in fact, that increasing the baffle length located between the hot sources always reduces the average Nusselt number of the lower source. This is because the baffle blocks the flow near it. Also, it is observed that the average Nusselt number always decreases with the increase in baffle length. In fact from $L_b = 0.2$ to $L_b = 0.6$ it decreases on average by 13.9% at the lower source and by 15.67% at the higher source. The maximum decrease is obtained for Ra = $6.51 \cdot 10^4$.

The full investigation of the square cavity with two baffles of different length will be experimentally and numerically investigated.

References

[1] C. J. Ho and J. Y. Chang, "A study of natural convection heat transfer in a vertical rectangular enclosure with two-dimensional discrete heating: effect of aspect ratio," *Int. J. Heat Mass Transfer*, 37 (6), pp. 917-925, 1994.

[2] H. Tűrkoglu and N. Yűcel, "Effects of heater and cooler location on natural convection in square cavities," *Numerical Heat Transfer*, Part A 27, pp. 351-358, 1995.

[3] N. Nithyadevi, N. P. Kandaswamy, and J. Lee, "Natural convection in a rectangular cavity with partially active side walls", *Int. J. Heat Mass Transfer*, 50, pp. 4688-4697, 2007.

[4] H. S. S. Chu, S. W. Churchill and S. V. Patterson, "The effects of heater size, location, aspect ratio and boundary conditions on two-dimensional, laminar, natural convection in rectangular channels," *ASME J. Heat Transfer*, 98, pp. 194-201, 1976.

[5] A. Valencia, and R.L. Frederick, "Heat transfer in square cavities with partially active vertical walls", *Int. J. Heat Mass Transfer*, 32 (8), pp. 1567-1574, 1989.

[6] Zhao, Liu et al., "Resonant response of fluid flow subjected to discrete heating elements", *Energy conversion and management*, 48, pp. 2461-2472, 2007.

[7] Qi-Hong Deng, "Fluid flow and heat transfer characteristics of natural convection in square cavities due to discrete source-sink pairs," *Int. J. of Heat and Mass Transfer*, 51, pp. 5949-5957, 2008.

[8] M. Paroncini, G. Nardini, "Heat transfer experiment on natural convection in a square cavity with discrete sources," *Heat and Mass Transfer*, 48, pp. 1855–1865, 2012, ISSN 0947-7411, DOI: 10.1007/s00231-012-1026-6.

[9] S. M. Bajorek and J. R. Lloyd, "Experimental investigation of natural convection in partitioned enclosures," *Journal of Heat Transfer*, 104, pp. 527-532, 1982.

[10] R. Jetli, S. Acharya, and E. Zimmerman, "Influence of the baffle location on natural convection in a partially divided enclosure," *Numerical Heat Transfer*, 10, pp. 521-536, 1986.

[11] H. Ambarita, K. Kishinami, M. Daimaruya, T. Saitoh, H. Takahashi, and J. Suzuki, "Laminar natural convection heat transfer in an air filled square cavity with two insulated baffles attached to its horizontal walls," *Thermal Science & Engineering*, vol. 14 n.3, pp. 35-46, 2006.

[12] S. H. Tasnim, and M. R. Collins, "Numerical analysis of heat transfer in a square cavity with a baffle on the hot wall," *Int. Comm. Heat Mass Transfer*, 31, p. 639-650, 2004.

[13] R. L. Frederick, "Natural convection in an inclined square enclosure with a partition attached to its cold wall," *Int. J. Mass Transfer*, 32, pp. 87-94, 1989.

[14] G. N. Facas, "Natural convection in a cavity with fins attached to both vertical walls", *J. Thermophys. Heat Transfer*, 7, pp.555-560, 1993.

[15] Y. Yamaguchi and Y. Asako, "Effects of partitions wall on natural convection heat transfer in a vertical air layer," *Journal of heat transfer*, 123, pp. 441-449, 2001.
[16] A. Nag, A. Sarkar, and V. M. K. Sastri, "Natural convection in a differentially heated square cavity with a horizontal partition plate on the hot wall," *Comput. Meth Appl. Mech. Eng*., 110, pp.143–156, 1993.
[17] X. Shi, and J. M. Khodadadi, "Laminar convection heat transfer in a differentially heated square cavity due to a thin fin on the hot wall," *J. Heat Transfer*, 125, pp. 624–634, 2003.
[18] M. Gassemi, M. Pirmohammadi, and Gh. A. Sheikhzadeh, "A numerical study of natural convection in a cavity with two baffles attached to its vertical walls," presented at the 2007 IASME/WEAS International Conference on Fluid Mechanics and Aerodynamics, Athens, Grece.
[19] E. Bilgen, "Natural convection in cavities with a thin fin on the hot wall," *Int. J. Heat and Mass Transfer*, 48, pp.3493-3505, 2005.
[20] W. Hauf, and U. Grigull, "Optical methods in heat transfer," in: *JP Harnett, TF Irvine Jr. (eds) Advances in Heat transfer*, New York: Academic Press, 1970, pp. 133–311. doi:10.1016/S0065-2717(08) 70151-5
[21] "FLUENT User's Guide", Fluent Incorporated